Free Radical Research, May 2011; 45(5): 620–637

RESEARCH ARTICLE

Protective role of a coumarin-derived schiff base scaffold against tertiary butyl hydroperoxide (TBHP)-induced oxidative impairment and cell death via MAPKs, NF-*k*B and mitochondria-dependent pathways

MANORANJAN GHOSH, PRASENJIT MANNA & PARAMES C. SIL

Division of Molecular Medicine, Bose Institute, P-1/12, CIT Scheme VII M, Kolkata-700054, India

(Received date: 24 November 2010; Accepted date: 31 January 2011)

Abstract

The present study investigated the antioxidant signalling mechanism of a coumarin-derived schiff base (CSB) scaffold against *tert*-butylhydroperoxide (TBHP) induced oxidative insult in murine hepatocytes. CSB possesses DPPH and other free radical scavenging activities. TBHP reduced cell viability and intracellular antioxidant status accompanied by an increase in intracellular ROS production in hepatocytes. TBHP also activated phospho-ERK1/2, phospho-p38 and NF-κB, altered the Bcl-2/Bad ratio, reduced mitochondrial membrane potential, released cytochrome C and activated caspase 3, suggesting that TBHP induced oxidative stress responsive cell death via apoptotic pathway. FACS analysis and DNA fragmentation studies also confirmed the apoptotic cell death in TBHP exposed hepatocytes. Treatment with CSB effectively reduced these adverse effects by preventing the oxidative insult, alteration in the redox-sensitive signalling cascades and mitochondrial events. Combining, results suggest that antioxidant property of CSB make the molecule to be a potential protective measure against oxidative insult, cytotoxicity and cell death.

Keywords: *Hepatocyte, TBHP, oxidative stress, cell death, MAPKs, CSB, antioxidant, cytoprotection*

Abbreviations: *ALT, alanine transaminase; CAT, catalase; CSB, Coumarin-derived schiff base; ERK, extracellular signal-regulated kinase; FACS, fluorescence activated cell sorting; GSH, glutathione; GSSG, glutathione disulphide; GST, glutathione-S-transferase; GPx, glutathione peroxidase; GR, glutathione reductase; MAPKs, mitogen activated protein kinases; MDA, malonaldehyde; NF-κB, nuclear factor kappa B; ROS, reactive oxygen species; RNS, reactive nitrogen species; SOD, superoxide dismutase; TBHP, tertiary butyl hydroperoxide.*

Introduction

Coumarins, the derivative of cinnamic acid with a benzo-α-pyrone [1,2] skeleton, are the widely distributed bioactive molecule in the plant kingdom. Recently these compounds have attracted much attention because of their broad range of biological activities such as anticancer, anti-oxidant, anti-inflammation, anti-HIV, anti-coagulant, antibacterial, analgesic and comparative immune-modulation [3–5]. Beside coumarins, schiff bases are also an important class of compounds in medicinal and pharmaceutical fields because of their wide range of biological applications including antibacterial [6], anti-fungal [7] and anti-tumour activities [8]. The active site of these compounds includes the azomethine group, which is the condensation product of primary amines and carbonyl groups. Thus, coumarin-derived schiff base molecules (CSBs) could be a source of drugs for the treatment of several diseases. Antioxidant and anti-inflammatory properties of some CSBs have already been reported by the earlier investigators [9–11]. However, there is no report describing the mechanism of the antioxidant and cytoprotective properties of CSBs.

Tertiary butyl hydroperoxide (TBHP) is a well known cytotoxin and oxidative agent, inducing oxidative stress in different organ systems including liver [12], testes [13], oocytes [14], retina [15], etc. This compound

Correspondence: Parames C. Sil, Professor, Division of Molecular Medicine, Bose Institute, P-1/12, CIT Scheme VII M, Calcutta-700054, West Bengal, India. Tel: 9133-25693243. Fax: 9133-2355-3886. Email: parames@bosemain.boseinst.ac.in; parames_95@yahoo.co.in

ISSN 1071-5762 print/ISSN 1029-2470 online © 2011 Informa UK, Ltd.
DOI: 10.3109/10715762.2011.564166

mainly acts by mobilization of arachidonic acid (AA) from membrane phospholipids in rat hepatocytes under cytotoxic conditions, thus leading to an increase in intracellular AA and malondialdehyde formation which precedes cell death. Although the exact mechanism of toxicity of this oxidative stress inducer is not clearly known, literature suggests the involvement of cellular lipids peroxidation, alkylation of cellular macromolecules like protein and DNA [16] and/or alterations in cellular calcium and glutathione levels [17]. In our laboratory we have previously investigated the involvement of TBHP-induced oxidative impairment and mechanism of cell death in isolated hepatocytes and found that the cytotoxic effect of TBHP is primarily due to increased production of ROS [18,19]. Several coumarin-derived Schiff bases have also been reported to posses antioxidant power [20]. It may, therefore, be logical to hypothesize that CSB could also play a protective role against TBHP-induced cytotoxicity.

In the present study we investigated the mechanism of action of CSB by determining, first, the radical scavenging activity of CSB (via DPPH assay) as well as superoxide and hydroxyl radical quenching ability in the cell free system. Second, dose- and time-dependent studies have been conducted to evaluate the optimum conditions necessary for CSB to exhibit its maximum protective action against TBHP-induced cellular oxidative damage by measuring the cell viability. Third, using that optimum dose and time, we determined its effect on the leakage of membrane-bound enzymes, activities of the antioxidant enzymes, cellular metabolites, lipid peroxidation, etc. After establishing its radical scavenging and antioxidative nature, we have carried out FACS analysis to investigate the mode of TBHP-induced cell death and its protection by CSB. Finally the mechanism of its protective action against TBHP-induced cellular damage and death by evaluating its effect on the alterations of MAPKs, NF-kB, Bcl-2 family proteins (Bcl-2 and Bad), mitochondrial membrane potential, cytosolic and mitochondrial cytochrome C, caspase 3 and cleaved caspase 3 activities. The results of the present study could clearly clarify the role of CSB in the protection of hepatocytes against oxidative insult induced by TBHP exposure.

Materials and methods

Materials

Bovine serum albumin (BSA), Bradford reagent, Collagenase type I, 2,2-diphenyl-1-picryl hydrazyl (DPPH), Dulbecco's modified Eagle's medium (DMEM), Foetal bovine serum (FBS) were purchased from Sigma-Aldrich Chemical Company (St. Louis, MO). Calcium chloride ($CaCl_2$), 1-chloro-2,4-dinitrobenzene (CDNB), dimethyl sulphoxide (DMSO), 5,5′-dithiobis (2-nitrobenzoic acid) [DTNB, (Ellman's reagent)], ethylene diamine tetraacetic acid (EDTA), glacial acetic acid, hydrogen peroxide (H_2O_2), N-ethylmaleimide (NEM), nicotinamide adenine dinucleotide reduced disodium salt (NADH), nitro blue tetrazolium chloride (NBT), oxidized glutathione (GSSG), phenazine methosulphate (PMT), potassium dihydrogen phosphate (KH_2PO_4), reduced glutathione (GSH), sodium azide (NaN_3) and thiobarbituric acid (TBA) were bought from Sisco Research Laboratory (Mumbai, India).

Synthesis of N-[(2-pyridyl)methyliden]-6-coumarin (CSB)

There are three steps in the preparation of CSB (Figure 1A): preparation of nitro coumarin (step 1), synthesis of aminocoumarin (step-2) and finally condensation of aminocoumarin with pyridine-2-carboxaldehyde to yield CSB (step-3).

Preparation of 6-nitrocoumarin (Step-1)

Coumarin was nitrated with mixed acid in an ice bath. Briefly, coumarin (8 gm, 54.8 mmol) was dissolved in conc. H_2SO_4 (40 cm^3) and temperature was maintained at -5°C and then 16 cm^3 mixed acid (HNO_3 and H_2SO_4 (conc.) in 1:3 volume ratio) was added. The mixture was stirred, kept at room temperature for 1 h and then to it ice was added. A white precipitate of 6-nitrocoumarin was obtained. It was then filtered and washed thorough with cold water (10 $cm^3 \times 10$) and dried over $CaCl_2$ and recrystallized from acetic acid. Yield was ~ 88% and the melting point was found to be 185 ± 2°C.

Synthesis of 6-aminocoumarin (Step-2)

Reduction of 6-nitrocoumarin was done using iron powder and ammonium chloride in water. 6-Nitrocoumarin (8 g, 41.9 mmol) in water (150 cm^3) was treated with Fe-powder (20 gm) and ammonium chloride (2.6 gm, 48.6 mmol). The mixture was kept in a water bath for 2 h with stirring. A dark brown precipitate was obtained which was then extracted with acetone. Evaporation of acetone yielded silky yellow precipitate of 6-aminocoumarin (m p 73°C). It was then recrystallized from dilute HCl solution as 6-aminocoumarin hydrochloride. Yield was ~ 76% and the melting point was found to be > 260°C.

Preparation of CSB (Step-3)

6-Aminocoumarine (0.5 g, 3.1 mmol) and pyridine-2-carboxaldehyde (0.26 ml, 3.1 mmol) were taken in dry methanol (15 cm^3) and refluxed for 8 h. After evaporation a straw colour crystalline compound was obtained. Yield was ~ 90% and the melting point was found to be 152 ± 2°C. Purity of the compound has been confirmed by using standard tools (like HPLC, Mass Spectroscopy and NMR (1H, 13C) studies).

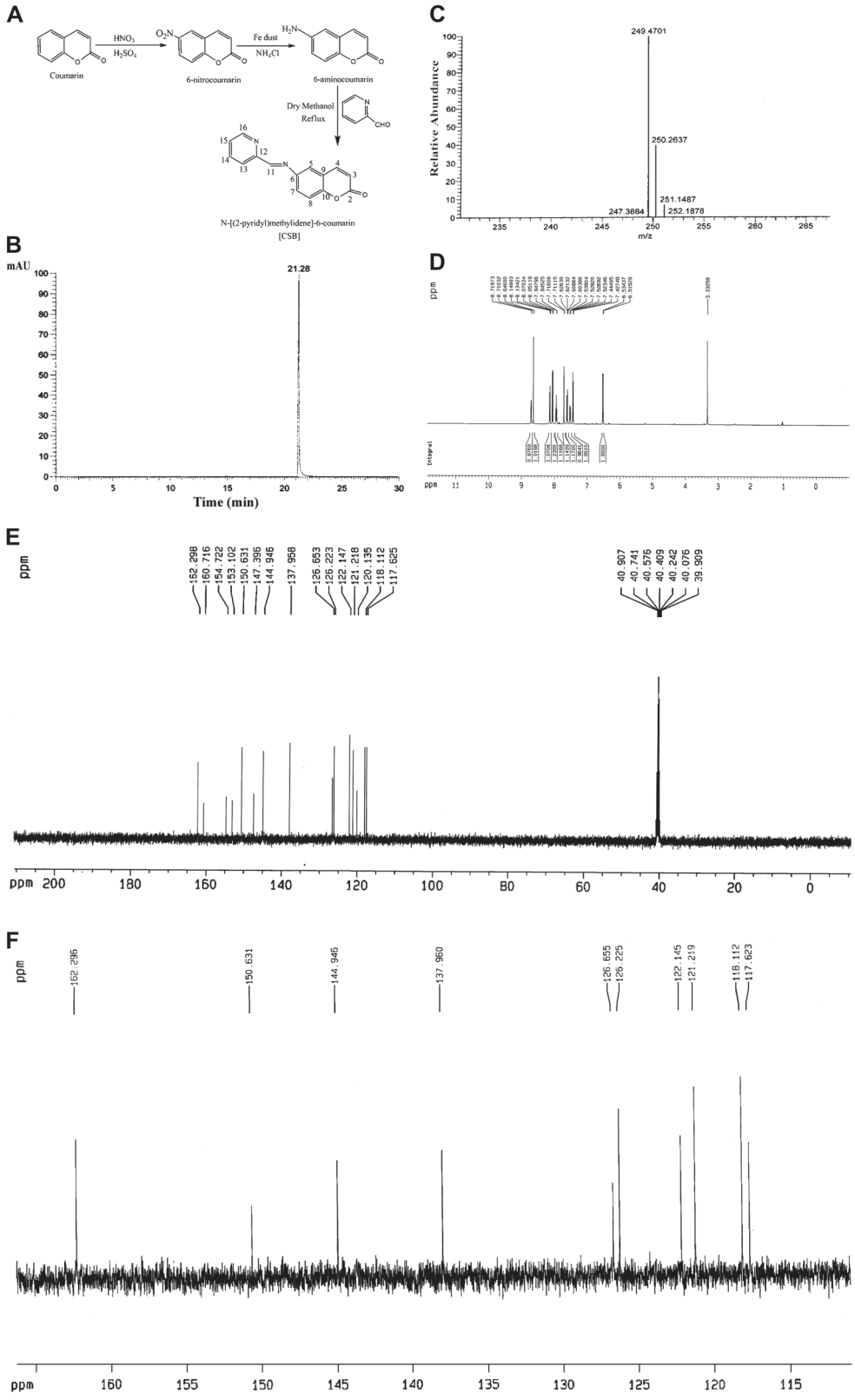

Figure 1. (A) Chemical synthesis of CSB. (B) Reverse phase HPLC analysis of CSB. (C) Mass spectra of the purified CSB; HRMS (ESI): m/z calculated ($C_{15}H_{10}N_2O_2$) 250.0742, found 249.4701 $[M]^+$. (D) ^1H NMR (500 MHz) spectra of CSB. (E) ^{13}C NMR (125 MHz) spectra of CSB. (F) Distortionless enhancement of polarization transfer using a 135° decoupler pulse (DEPT-135) spectra of CSB.

NMR studies of CSB

To perform the NMR study, 15 mg of CSB was dissolved in 0.6 ml of DMSO-d_6 in a NMR tube. The ^{1}H NMR spectrum (500 MHz) of CSB was recorded on a Bruker Avance DRX 500 spectrometer (tetramethylsilane (for ^{1}H, δ = 0.00 ppm) as internal standard). For ^{13}C NMR (125 MHz) spectrum, 25 mg of CSB was dissolved in 0.6 ml of DMSO-d_6 and the spectrum was recorded on a Bruker Avance DRX 500 spectrometer ((DMSO, δ = 40.4 ppm) as internal standard). The following abbreviations were used to explain the multiplicities: s = singlet, d = doublet, t = triplet, m = multiplet, br = broad and J = coupling constant in Hz.

Antioxidant activity of CSB in cell free system

DPPH radical quenching activity. The antioxidant activity of CSB was measured using the DPPH radical as described by Blois [21]. Two millilitres of DPPH solutions (125 μM) in methanol and 2 ml of tested samples with different concentrations (0.4, 2, 4, 6, 8, 10, 12, 16, 20, 24 and 28 mM) of CSB were mixed in the tubes. The solution was shaken and incubated at 37°C for 30 min in the dark. The decrease in absorbance at 517 nm was measured against methanol blank using a UV/Visible spectrophotometer. Percentage inhibition was calculated by comparing the absorbance values of control and the sample.

$$\text{Percentage inhibition} = \frac{A_1 - A_2}{A_1} \times 100$$

where A_1 is the absorbance of the blank and A_2 is the absorbance in the presence of CSB.

Hydroxyl radical scavenging activity. The hydroxyl radical scavenging activity of CSB has been investigated following the method of Nash [22] using the same concentrations of CSB as mentioned above. *In vitro* hydroxyl radicals were generated by Fe^{3+}/ascorbic acid system. The detection of hydroxyl radicals was carried out by measuring the amount of formaldehyde produced from the oxidation of dimethyl sulphoxide (DMSO). The formaldehyde produced was detected spectrophotometrically at 412 nm.

Superoxide radical scavenging activity. The superoxide radical scavenging activity was measured following the method of Siddhuraju and Becker [23]. The reaction mixture contained 0.1 M phosphate buffer, pH 7.4, 150 μM nitroblue tetrazolium (NBT), 60 μM phenazine methosulphate (PMT), 468 μM NADH and different concentrations of CSB (as mentioned earlier). The mixture was incubated in the dark for 10 min at 25°C and the absorbance was read at 560 nm. Results were expressed as percentage inhibition of the superoxide radicals.

Hepatocyte isolation

For the present study, hepatocytes were aseptically isolated from mice livers following the modified method as described previously by Sarkar and Sil [24]. Briefly, the livers were isolated under aseptic conditions, placed in phosphate buffer saline, irrigated in buffer A (10 mM HEPES, 3mM KCl, 130 mM NaCl, 1 mM NaH_2PO_4-H_2O and 10 mM glucose, pH 7.4) and then incubated in buffer B (5 mM $CaCl_2$, 0.03% collagenase type I) for ~ 45 min at 37°C. The tissue was passed through a wide bore syringe and 80 μm decron mesh, respectively. The dissociated cells were centrifuged at 500xg and the pellet was suspended in Dulbecco's minimal essential medium (DMEM) containing 10% foetal calf serum and 5 μg/ml insulin, 5 μM hydrocortisone, 100 U/ml penicillin and 100 μg/ml streptomycin. The suspension was adjusted to obtain ~ 2×10^6 cells/ml.

Determination of hepatocyte viability

Viability of hepatocytes was determined by MTT assay [25]. After treatments, cells were incubated with 500 μg/ml 3-(4,5-dimethyl-thiazol-2-yl) 2,5-diphenyltetrazolium bromide (MTT) for 4 h. The functional mitochondrial succinate dehydrogenases in survival cells can convert MTT to formazan that generates a blue colour. At last the formazan was dissolved in 10% SDS–5% isobutanol–0.01 M HCl. The optical density was measured at 570 nm with 630 nm as a reference and cell viability was normalized as a percentage of control.

Determination of time and dose-dependent effect of TBHP

Time- and dose-dependent effects of TBHP were determined by cell viability assessment. Briefly, for dose-dependent study, eight different sets of hepatocytes, each containing ~ 2×10^6 cells, were incubated with eight different doses of TBHP (50, 100, 200, 300, 400, 500, 600 and 700 μM) for 3 h to determine the maximum damage caused by TBHP treatment. For time-dependent study, six different sets of hepatocytes (1 ml cell suspension ~ 2×10^6 in each) were exposed to TBHP (500 μM) for different times (30 min, 1 h, 1.5 h, 2 h, 2.5 h and 3 h). The resulting cells were rinsed and incubated with 0.5% FBS–DMEM medium containing MTT (5 mg/ml) for 4 h. At the end of the incubation period the medium was removed and the converted dye was solublized with DMSO (0.3 ml). Absorbance was measured at 570 nm and cell viability was expressed as a percentage of the corresponding control.

Assessment of dose- and time-dependent activity of CSB

Cell viability assessment has been carried out to determine the optimum dose and time of CSB needed for the cytoprotection against TBHP-induced cytopathophysiology. Briefly, for dose-dependent study, six

different sets of hepatocytes, each containing ~ 2×10^6 cells were exposed to 500 μM TBHP along with CSB (0.1, 0.2, 0.4, 0.8, 1.0 and 1.2 mM) for 2 h. For time-dependent study, six different sets of hepatocytes (1 ml cell suspension ~ 2×10^6 in each) were incubated with CSB (0.8 mM) for different times (30 min, 1 h, 1.5 h, 2 h, 2.5 h and 3 h). The cell viability was determined and expressed as described above.

Experimental set-up

Based on the results of the dose- and time-dependent effects of both TBHP and CSB, we designed the *in vitro* experiments with different sets of hepatocytes containing 1 ml suspension (~ 2×10^6 cells) in each. Cells were incubated in a CO_2 incubator at 37°C throughout the experiment with gentle shaking. The hepatocytes kept in culture medium only served as normal control (marked as 'Cont'). Hepatocytes (~ 2×10^6 cells) incubated with CSB (0.8 mM) alone for 2 h served as a group showing the effect of CSB on hepatocytes (marked as 'CSB'). Hepatocytes (~ 2×10^6 cells) incubated with 500 μM TBHP for 2 h served as toxin control (marked as 'TBHP'). For the pre-treatment studies, hepatocytes (~ 2×10^6 cells) were incubated with CSB (0.8 mM) for 30 min prior to TBHP exposure and were incubated further for 2 h (marked as 'CSB + TBHP'). The combined effect of CSB and TBHP was studied by incubating the cells with these agents together for 2 h (marked as 'CSB& TBHP'). Positive control cells were prepared by incubating hepatocytes with vitamin C (100 mg/ml) instead of CSB (marked as 'TBHP + VitC'). For all the subsequent experiments (results, figures, tables, etc.) the above notations would be used if not mentioned otherwise.

Determination of ALT and LDH leakage

The leakage of the enzymes, ALT and LDH is associated with cell viability and is considered as an important indicator of cellular membrane damage. After appropriate experimental procedure as described earlier, hepatocyte suspensions were centrifuged at 60 g. The leakage of ALT and LDH (secreted outside the cells) was determined from the supernatant using a kit (Span Diagnostics Ltd., Surat, India).

Determination of protein content

The protein content was measured by the method of Bradford [26] using crystalline BSA as standard.

Determination of intracellular ROS production

ROS plays a major role in TBHP-induced hepatic dysfunction and hepatocellular death. In the present study, intracellular ROS production was estimated by using 2,7-dichlorofluorescein diacetate (DCFDA) as a probe following the method of LeBel and Bondy [27] as modified by Kim et al. [28]. DCF-DA diffuses through the cell membrane where it is enzymatically deacetylated by intracellular esterases to the more hydrophilic non-fluorescent reduced dye dichlorofluorescin. In the presence of reactive oxygen metabolites, non-fluorescent DCFH rapidly oxidized to highly fluorescent product DCF. After performing the experiments (as described in the experimental set-up) hepatocytes were incubated with the assay media (20 mM tris-HCl, 130 mM KCl, 5 mM $MgCl_2$, 20 mM NaH_2PO_4, 30 mM glucose and 5 μM DCFDA) at 37°C for 15 min. The formation of DCF was measured at the excitation wavelength of 488 nm and emission wavelength of 510 nm for 10 min by using a fluorescence spectrometer (HITACHI, Model No F4500) equipped with a FITC filter.

Lipid peroxidation and protein carbonylation estimation

The extent of lipid peroxidation in terms of malondialdehyde (MDA) formation was measured according to the method of Esterbauer and Cheeseman [29]. Sample containing1 mg protein was mixed with 1 ml TCA (20%), 2 ml TBA (0.67%) and heated for 1 h at 100°C. After cooling, the precipitate was removed by centrifugation. The absorbance of the sample was measured at 535 nm using a blank containing all the reagents except the sample. MDA content of the sample was calculated using the extinction co-efficient of MDA, which is 1.56×10^5 $M^{-1}cm^{-1}$.

Protein carbonyl contents were determined according to the methods of Uchida and Stadtman [30]. The sample was treated with an equal volume of 0.1% (w/v) 2,4-DNPH in 2 N HCl and incubated for 1 h at room temperature and then treated with 20% TCA. After centrifugation, the precipitate was extracted three times with EtOH/EtOAc and dissolved in 8 M guanidine hydrochloride in 133 mM tris solution containing 13 mM EDTA. The absorbance was recorded at 365 nm. The results were expressed as nmol of DNPH incorporated/mg protein based on the molar extinction coefficient of 22 000 $M^{-1}cm^{-1}$ for aliphatic hydrazones.

Antioxidant enzymatic activities assay

The activities of antioxidant enzymes, superoxide dismutase (SOD), catalase (CAT), glutathione-S-transferase (GST), glutathione reductase (GR) and glutathione peroxidase (GPx) were measured in all experimental sets following the method of Sinha et al. [31].

Briefly, in case of SOD assay tissue homogenates were centrifuged at 600 g for 8 min at 4°C. Supernatants were decanted and re-centrifuged at 5500 g for 15 min to form mitochondrial pellets. The supernatant

was kept as 'cytosolic fraction'. Five micrograms of protein of the cytosolic fraction was mixed with sodium pyrophosphate buffer, PMT and NBT. The reaction was started by the addition of NADH. Then the reaction mixture was incubated at 30°C for 90 s and stopped by the addition of 1 ml of glacial acetic acid. The absorbance of the chromogen formed was measured at 560 nm. One unit of SOD activity is defined as the enzyme concentration required to inhibit chromogen production by 50% in 1 min under the assay condition.

CAT activity was determined by following the decomposition of H_2O_2 (7.5 mM) at 240 nm for 10 min and it was monitored spectrophotometrically. One unit of CAT activity is defined as the amount of enzyme which reduces 1 μmol of H_2O_2 per minute.

GST activity was assayed based on the conjugation reaction with glutathione in the first step of mercapturic acid synthesis. The reaction mixture contains supernatant 25 μg protein sample, KH_2PO_4 buffer, EDTA, CDNB and GSH. The reaction was carried out at 37°C and monitored spectrophotometrically at 340 nm for 5 min. One unit of GST activity is 1 μmol product formation per minute.

GR activity was determined spectrophotometrically by monitoring the absorbance at 412 nm for 3 min at 24°C. Reaction mixture contained 1 mM EDTA, 0.3 mM DTNB, 2 mM NADPH and 20 mM GSSG. The enzyme activity was calculated using a molar extinction coefficient of 13 600 $M^{-1}cm^{-1}$. One unit of enzyme activity is defined as the amount of enzyme, which catalyses the oxidation of 1 μmol NADPH per minute.

GPx activity was measured by using H_2O_2 and NADPH as substrates. The conversion of NADPH to $NADP^+$ was observed by recording the changes in absorption intensity at 340 nm and one unit of enzyme activity is defined as the amount of enzyme that catalyses the oxidation of 1 μmol NADPH per minute.

Measurement of cellular glutathione and glutathione disulphide

The levels of cellular glutathione (GSH) and glutathione disulphide (GSSG) were determined by the DTNB assay according to the method of Ji et al. [32]. Briefly, after treatment cells were harvested with metaphosphoric acid (5%) buffer. The reaction mixture contained 1 mM EDTA, NADPH (0.24 mM), glutathione reductase (0.06 U), DTNB (86 mM) and samples. Yellow coloured 5-thio-2-nitrobenzoic acid (TNB) formation is monitored at 412 nm. GSSG was determined after elimination of GSH with 1-methyl-2-vinylpyridinium trifluoromethanesulphonate (M2VP). The levels of GSH were calculated from the difference between concentrations of total glutathione (GSH + GSSG) and GSSG. The intracellular levels of GSH and GSSG were calculated based on cellular protein concentration.

Isolation of nuclear fraction of hepatocytes

All sets of experimental hepatocytes were sonicated and then centrifuged at 600 g for 10 min at 5°C in a centrifuge. The nuclear extract was prepared according to a modified method of Tapalaga et al. [33]. The pellet obtained was resuspended in buffer C (250 mM sucrose, 5 mM $MgCl_2$, 10 mM Tris-HCl, pH 7.4) and again centrifuged at 600 g at 5°C for 10 min. This pellet of crude nuclei obtained after the second centrifugation was resuspended in nine volumes of buffer D (2.2 M sucrose, 1 mM $MgCl_2$, 10 mM Tris-HCl, pH 7.4) and centrifuged at 70 000 g at 4°C for 80 min in a ultracentrifuge. The purified nuclei were resuspended in buffer C.

Immunoblotting

An equal amount of protein (50 μg) from each sample was resolved by 10% SDS-PAGE and transferred to PVDF membrane. Membranes were blocked at room temperature for 2 h in blocking buffer containing 5% non-fat dry milk to prevent non-specific binding and then incubated with anti p-38 (1:1000 dilution), anti p-ERK1/2 (1:1000 dilution), anti Bad (1:1000 dilution), anti Bcl-2 (1:1000 dilution), anti p-NF-kB (serine 276) (1:250 dilution), anti p-IKK*α*/*β* (1:1000 dilution), anti IkB*α* (1:1000 dilution) and anti cleaved-caspase3 (1:100 dilution) primary antibodies separately at 4°C overnight. The membranes were washed in TBST (50 mmol/L Tris-HCl, pH 7.6, 150 mmol/L NaCl, 0.1% Tween 20) for 30 min and incubated with appropriate HRP conjugated secondary antibody (1:2000 dilution) for 2 h at room temperature and developed by the HRP substrate 3,3'-diaminobenzidine tetrahydrochloride (DAB) system (Bangalore genei, India).

Isolation of mitochondria from liver tissue and determination of mitochondrial membrane potential($\Delta\psi_m$)

After performing the experiments (as described in the experimental set-up), mitochondrial membrane potential ($\Delta\psi_m$) was estimated on the basis of cell retention of the fluorescent cationic probe rhodamine 123 [34]. Briefly, the mitochondrial suspension was incubated with 1 μM rhodamine 123 for 10 min, centrifuged at 50x*g* for 5 min at 4°C, washed and resuspended in 1 mL of 0.1% Triton X-100. After centrifugation at 2000x*g* for 5 min, fluorescence of rhodamine 123 was determined using a BD-LSR flow cytometer. Cell debris, characterized by a low FSC/SSC, was excluded from analysis. The data was analysed by Cell Quest software**.** In this assay carbonyl cyanide m-chlorophenyl

hydrazone (CCCP) (1 µl of 50 mM CCCP per 1 ml cell suspension) was used as a positive control.

Cytochrome C determination by western blotting

To determine the levels of cytochrome C, the mitochondrial fractions were used. These fractions were subjected to immunoblot analysis as described above.

DNA fragmentation analysis

The extent of DNA fragmentation has been assayed by electrophoresing the DNA samples on agarose/ethydium bromide gel. DNA samples were isolated from the hepatocytes of different experimental sets using the kit (MO BIO Laboratories, Carlsbad, CA).

Detection of the nature of cell death by flow cytometry (FACS)

Dual parameter FACS analysis allows for the discrimination between viable, apoptotic and necrotic cells. After appropriate treatments (as described in the experimental set-up), hepatocytes were washed with PBS, centrifuged at 800 g for 6 min, resuspended in ice-cold 70% ethanol/PBS, centrifuged at 800 g for a further 6 min and resuspended in PBS. Cells were then incubated with PI and FITC-labelled Annexin V for 30 min at 37°C. Excess PI and Annexin V were then washed off; cells were fixed and then stained cells were analysed by flow cytometry using FACS Calibur (Becton Dickinson, Mountain View, CA) equipped with 488 nm argon laser light source; 515 nm band pass filter for FITC-fluorescence and 623 nm band pass filter for PI-fluorescence using CellQuest software. A dot plot of PI-fluorescence (*y*-axis) vs FITC-fluorescence (*x*-axis) has been prepared.

Statistical analysis

All the values are expressed as mean ± SD ($n = 6$). Significant differences between the groups were determined with SPSS 10.0 software (SPSS Inc., Chicago, IL) for Windows using one-way analysis of variance (ANOVA) and the group means were compared by Student-Newman-Keuls post-hoc tests. A difference was considered significant at the $p < 0.05$ level.

Results

Figure 1A represents the routes of the chemical synthesis of CSB. Figure 1B represents the reverse phase HPLC chromatograph of CSB. In this figure a single peak appeared with the retention time of 21.28 min confirming its homogeneous preparation and absence of any contaminating substances. Figure 1C shows the Mass Spectra of the purified CSB. High resolution mass spectroscopy (HRMS) spectrum also supports the purity of CSB. HRMS (ESI): m/z calculated 250.0742 $[M]^+$ and found m/z 249.4701 $[M]^+$ unambiguously confirms the purity of CSB as a single compound.

Results of ^{1}H NMR spectrum of pure CSB has been represented in Figure 1D. ^{1}H NMR (500 MHz, DMSO-d_6) δ 6.52 (3-H, d, J = 9.5 Hz), 8.06 (4-H, d, J = 9.5 Hz), 7.61 (5-H, m), 7.52 (7-H, m), 7.44 (8-H, d, J = 8.7 Hz), 8.64 (11-H, s), 8.14 (13-H, d, J = 7.8 Hz), 7.94 (14-H, m), 7.71 (15-H, d, J = 2.5 Hz), 8.71 (16-H, d, J = 4.7 Hz).

Figure 1E shows the ^{13}C NMR spectrum of pure CSB. ^{13}C NMR (125 MHz, DMSO-d_6) δ 162.29 (C-2), 117.62 (C-3), 144.94 (C-4), 118.11 (C-5), 147.39 (C-6), 122.14 (C-7), 120.13 (C-8), 121.21 (C-9), 154.72 (C-10), 160.71 (C-11), 150.63 (C-12), 137.95 (C-13), 126.65 (C-14), 126.21 (C-15), 153.10 (C-16).

The results from ^{13}C NMR spectrum are also supported by Distortionless Enhancement of Polarization Transfer using a 135° decoupler pulse (DEPT-135) analysis. Figure 1F shows the DEPT-135 ^{13}C NMR spectra of pure CSB. This pulse sequence produces a carbon spectrum with methyl (CH_3) and tertiary (CH) carbons up and methylene (CH_2) carbons down.

Combining all, our spectral data analysis suggests that the preparation of CSB is homogenous and pure.

Free radical scavenging activities of CSB in cell-free system

Effect on DPPH radical quenching. The DPPH radical scavenging effect of CSB has been shown in Figure 2A. It has been observed that with an increase in concentration of CSB the colour of the DPPH radical vanishes rapidly at 517 nm. The maximum DPPH radical quenching was observed when CSB was incubated at a concentration of 20 mM with DPPH solution. Hence, it can be anticipated that the compound possesses potent DPPH radical scavenging activity.

Hydroxyl ($OH^{\cdot}$) and Super oxide ($O_2^{\cdot}$) radicals scavenging power. Figure 2B represents the hydroxyl and superoxide radicals scavenging activity of CSB in a cell free system. It has been observed that at a dose of 16 mM, CSB shows maximum superoxide radical ($O_2^{\cdot}$) scavenging activity. However, the optimum hydroxyl radical ($OH^{\cdot}$) scavenging power was observed when CSB was incubated at a concentration of 10 mM.

Dose- and time-dependent effect of TBHP-induced cytotoxicity

Assessment of cell viability is an important indicator of finding the degree of cytotoxicity, caused by any xenobiotics. Figure 3A depicts the dose- and time-dependent effect of TBHP in murine hepatocytes.

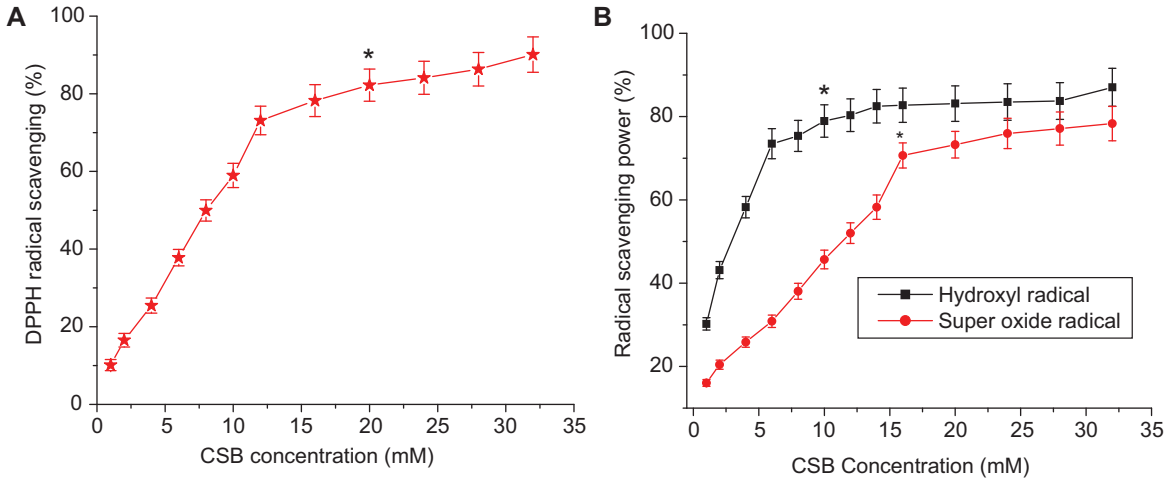

Figure 2. Free radical scavenging activities of CSB in cell free system. (A) The DPPH radical scavenging, (B) the hydroxyl and superoxide radical scavenging activities. Values are represented as the mean of six different experiments in each set. Data represent the average ± SD of six separate experiments. * sign indicates the optimum dose of CSB at which it shows its significant radical scavenging activity.

TBHP caused a reduction in cell viability linearly at a dose of 500 µM when exposed for 2 h. The effect of TBHP remained practically unaltered beyond this concentration and time. For all the subsequent experiments in this particular study, this dose (500 µM) and incubation time (2 h) of TBHP has been taken as optimum.

Dose- and time-dependent effect of CSB against TBHP-mediated cellular damage

Results of the dose- and time-dependent effects of CSB against TBHP-induced oxidative impairment in murine hepatocytes have been summarized in Figure 3B. TBHP exposure caused reduction in cell viability at a dose of 500 µM when incubation was carried out for 2 h. In order to determine whether this loss could be prevented by CSB treatment, we performed MTT assay. Incubation of the hepatocytes with CSB (prior to TBHP exposure) linearly prevented the reduction in cell viability up to a dose of 800 µM for 2 h and this effect of CSB remained practically unaltered beyond this concentration and time period. For all the subsequent experiments in this particular study, this dose (800 µM) and time (2 h) of CSB have been taken as optimum.

Effect on membrane bound enzymes

ALT and LDH leakage are associated with cell viability and is considered as an important indicator of cellular membrane damage. Severe leakage of these membrane bound enzymes were found in the TBHP-treated hepatocytes indicating that the loss of cell membrane integrity and cytotoxicity were caused by TBHP on hepatocytes (Figure 4A). Treatment with CSB either prior to or simultaneous with the TBHP exposure effectively inhibited the TBHP-induced membrane disruption caused, as revealed from the lower ALT and LDH levels outside the cells.

Effects on levels of lipid peroxidation and protein carbonyl content

Lipid peroxidation and protein carbonylation are widely used as the marker of cell membrane damage and oxidative modification of proteins, respectively. In the present study the lipid peroxidation has been measured by estimating the concentration of MDA (lipid peroxidation end product). TBHP intoxication increased the levels of MDA and protein carbonylation in hepatocytes (Figure 4B). Treatment with CSB has been found to be effective in preventing the TBHP-induced lipid peroxidation and protein carbonylation.

Effects on the ratio of GSH and GSSG

GSH plays a critical role in scavenging intracellular reactive intermediates. A massive amount of GSH is consumed to accomplish this task, thus shifting the redox status of the cell. Whenever the GSH level decreases below the threshold level, the concentration of reactive radicals gets elevated and causes oxidative stress. During oxidative stress GSH is oxidized to GSSG that may reacts with the –SH groups of proteins forming mixed disulphide through thiol/disulphide exchange. In the present study, intracellular redox status was greatly impaired by TBHP exposure, as manifested by a significant decrease in the levels of GSH along with the increased level of GSSG and, thus, the GSH/GSSG ratio suggesting that the non-protein sulphydyl groups and protein-bound sulphydryl groups could alter each other via thiol/disulphide exchange (Figure 4C). Treatment with CSB either prior to or

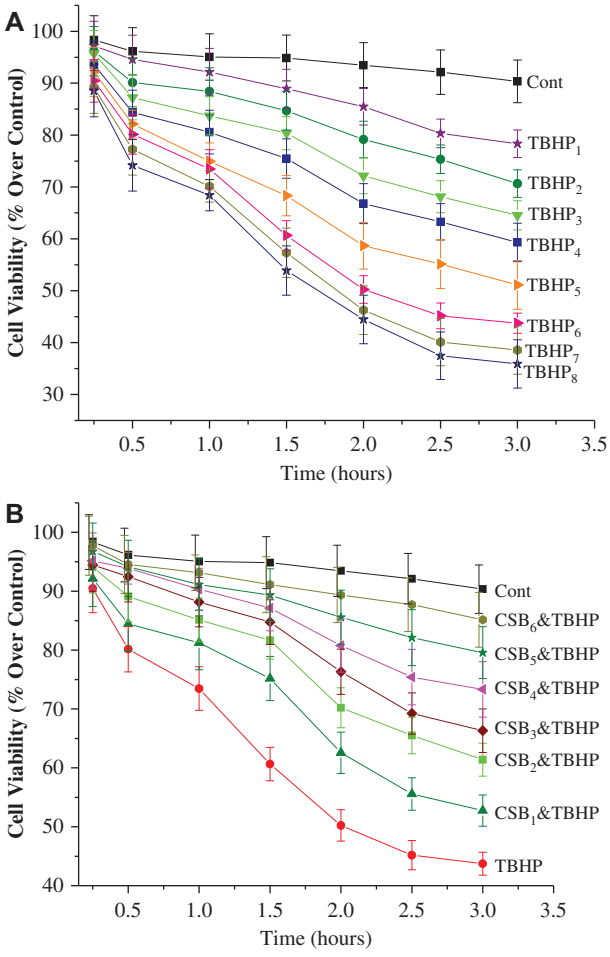

Figure 3. (A) Time- and dose-dependent effect of TBHP-induced loss in cell viability. Values are expressed as percentage over control. Cont: Time-dependent cell viability of the normal hepatocytes incubated in DMEM up to 180 min. $TBHP_1$-$TBHP_8$: Time-dependent cell viability when hepatocytes were incubated with TBHP (50, 100, 200, 300, 400, 500, 600 and 700 μM) in DMEM up to 180 min. Data are mean ± SD, for six separate experiments per group and were analysed by one-way ANOVA, with Student-Newman-Keuls post-hoc tests. (B) Time- and dose-dependent prevention of the TBHP-induced loss in cell viability by CSB. Values are expressed as percentage over control. Cont: Time-dependent cell viability of the normal hepatocytes incubated in DMEM up to 180 min. TBHP: Time-dependent cell viability when hepatocytes were incubated with TBHP (500 μM) in DMEM up to 180 min. CSB_1&TBHP-CSB_6&TBHP: Time-dependent cell viability when hepatocytes were incubated with CSB (0.1, 0.2, 0.4, 0.8, 1.0 and 1.2 mM) simultaneously with TBHP (500 μM) in DMEM up to 180 min. Data are mean ± SD, for six separate experiments per group and were analysed by one-way ANOVA, with Student-Newman-Keuls post-hoc tests.

simultaneous with the TBHP exposure could, however, prevent these alterations.

Effect of intracellular ROS production

Intracellular ROS production plays an important role in TBHP-induced oxidative impairments. Figure 5 represents the levels of intracellular ROS in the normal and experimental hepatocytes. It has been observed that TBHP exposure caused increased production of

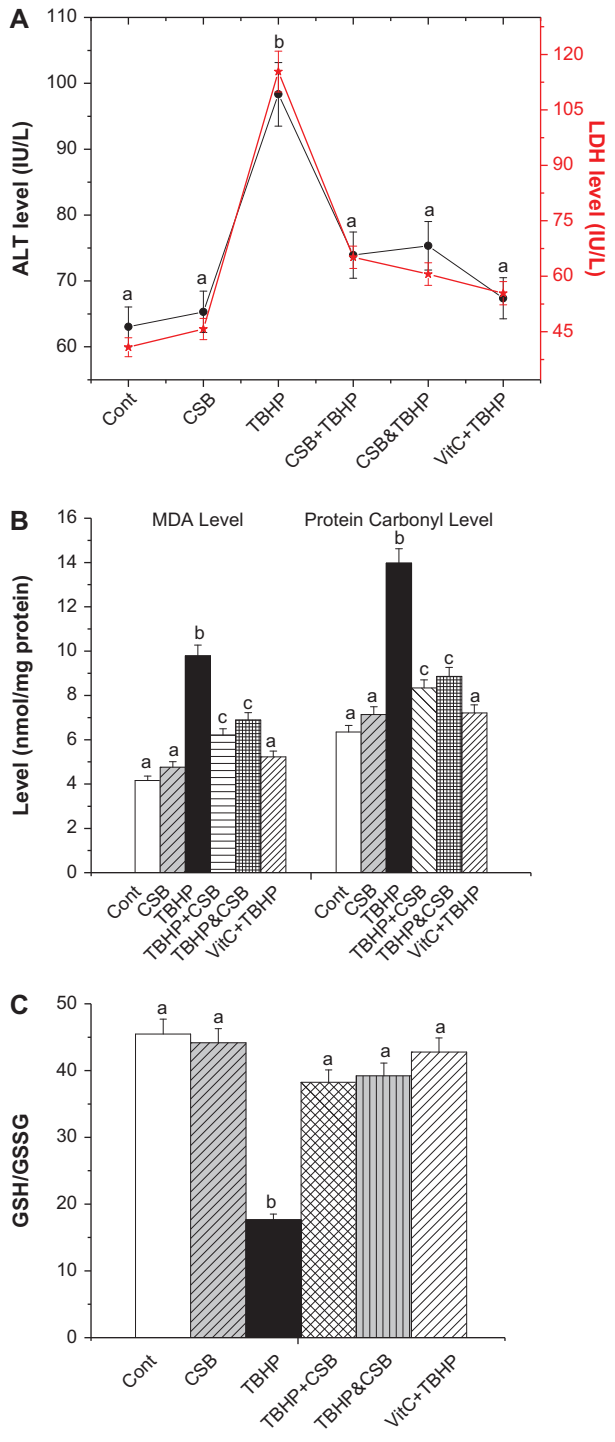

Figure 4. Effect of CSB and TBHP on the levels of membrane leakage enzymes (ALT and LDH) (A), levels of lipid peroxidation as well as protein carbonylation (B) and ratio of GSH/GSSG (C). Cont: level in normal hepatocytes, CSB: level in hepatocytes treated with CSB, TBHP: level in only TBHP-exposed hepatocytes, CSB + TBHP: level in hepatocytes treated with CSB prior to TBHP addition, CSB&TBHP: level in hepatocytes exposed to CSB and TBHP simultaneously, VitC + TBHP: level in hepatocytes treated with vitamin C prior to TBHP exposure. Data are mean ± SD, for six sets per group and were analysed by one-way ANOVA, with Student-Newman-Keuls post-hoc tests. Differences were attributed at $p < 0.05$ and homogeneous sub-groups share common superscripted letters.

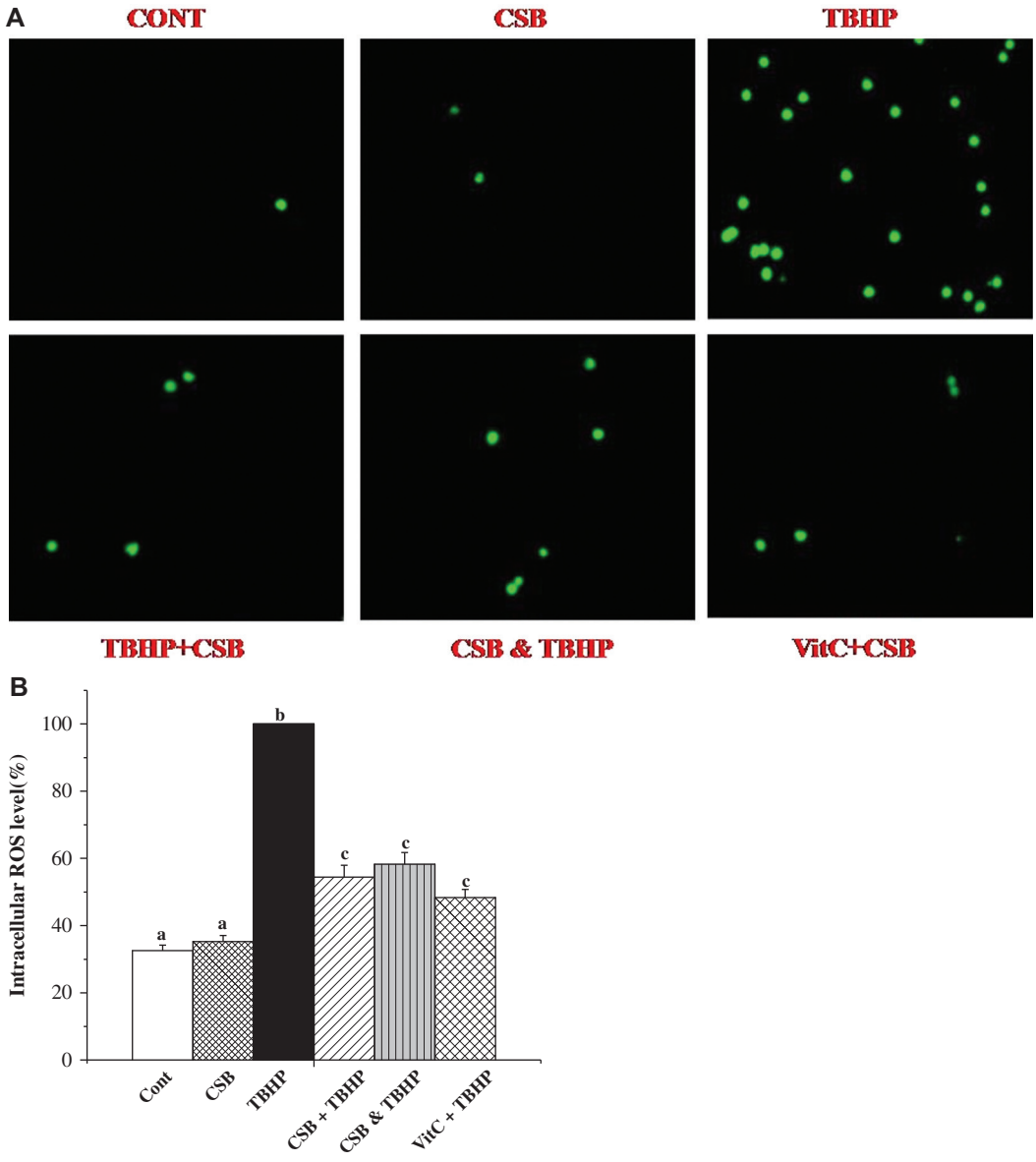

Figure 5. Effect of CSB on TBHP-induced intracellular ROS production in hepatocytes. (A) Representative images under fluroscence microscope (original magnification 400 ×), (B) Intracellular ROS levels was detected by DCF-DA method. Cont: ROS level in normal hepatocytes, CSB: ROS level in hepatocytes treated with CSB, TBHP: ROS level in only TBHP exposed hepatocytes, CSB + TBHP: ROS level in hepatocytes treated with CSB prior to TBHP addition, CSB&TBHP: ROS level in hepatocytes exposed to CSB and TBHP simultaneously, VitC + TBHP: ROS level in hepatocytes treated with vitamin C prior to TBHP exposure. Data are mean ± SD, for six sets per group and were analysed by one-way ANOVA, with Student-Newman-Keuls post-hoc tests. Differences were attributed at $p < 0.05$ and homogeneous sub-groups share common superscripted letters.

intracellular ROS and that could be prevented by the treatment with CSB either prior to or simultaneous incubation with TBHP.

Effect on the activities of antioxidant enzymes

Oxidative stress is the result of a redox imbalance between the generation of ROS and the compensatory response from the endogenous antioxidant network. To investigate whether the radical scavenging activity of CSB was mediated by the activities of antioxidant enzymes, we have measured the activities of intracellular antioxidant enzymes, SOD, CAT, GST, GR and GPx. Table I represents the activities of the antioxidant enzymes in normal and experimental hepatocytes. Our study reveals that TBHP significantly attenuated the activities of the antioxidant enzymes. Results suggest that prior or simultaneous treatment with CSB could be able to prevent the reduction in the antioxidant enzymes activities.

Effect on the mitogen-activated protein kinase (MAPKs) cascades

MAPKs are the upstream critical signalling proteins. They can be classified into three distinct

Table I. Effect of tertiary butyl hydroperoxide (TBHP) and CSB on the activities of the antioxidant enzymes in the normal and experimental hepatocytes.

Name of the antioxidant enzymes	Activities of the antioxidant enzymes					
	Normal control	CSB treated	TBHP treated	CSB + TBHP	CSB & TBHP	VitC + TBHP
SOD (Unit/mg protein)	74.55 ± 3.64[a]	73.17 ± 3.73[a]	38.78 ± 1.81[b]	68.37 ± 3.54[a]	70.14 ± 3.43[a]	72.49 ± 3.64[a]
CAT (μmol/min/mg protein)	208.34 ± 10.21[a]	204.29 ± 9.89[a]	156.87 ± 7.47[b]	180.45 ± 9.25[a]	183.34 ± 8.79[a]	198.35 ± 9.82[a]
GST (μmol/min/mg protein)	0.42 ± 0.02[a]	0.39 ± 0.02[a]	0.15 ± 0.007[b]	0.24 ± 0.01[c]	0.27 ± 0.01[c]	0.34 ± 0.02[a]
GR (nmol/min/mg protein)	216.73 ± 10.12[a]	213.83 ± 9.76[a]	86.74 ± 4.19[b]	149.28 ± 7.33[c]	146.34 ± 7.29[c]	171.25 ± 8.37[c]
GPx (nmol/min/mg protein)	161.21 ± 7.9[a]	158.43 ± 7.81[a]	87.38 ± 4.29[b]	131.28 ± 6.48[a]	129.14 ± 6.28[a]	149.34 ± 7.37[a]

[a]Values normal control ($P^a<0.05$).
[b]Values differ significantly from normal control ($P^b<0.05$).
[c]Values differ significantly from b ($P^c<0.05$).
Normal control: normal hepatocytes; CSB treated: hepatocytes treated with CSB; TBHP treated: hepatocytes treated with TBHP; CSB + TBHP: hepatocytes treated with CSB followed by TBHP exposure; CSB & TBHP: hepatocytes treated with CSB and TBHP simultaneously; and VitC + TBHP: hepatocytes treated with vitamin C followed by TBHP exposure. Data are mean ± SD, for six sets per group and were analysed by one-way ANOVA, with Student-Newman-Keuls post-hoc tests. Differences were attributed at $p < 0.05$, and homogeneous sub-groups share common superscripted letters A.

sub-families: extracellular signal-regulated protein kinase (ERK1/2), p38-MAPK (p38) and c-Jun N-terminal kinase (JNK). In our study we investigated the effect of CSB against TBHP-induced expression of MAPKs proteins (ERK1/2, p38 and JNK) (Figure 6). It has been observed that TBHP exposure increased the expressions of phosphorylated p38 as well as ERK1/2 (without any change in phosphorylated JNK) and that could be prevented by the treatment of CSB either prior to or simultaneous incubation with the TBHP.

Effect on the phosphorylation of IKKα/β, NF-κB and degredation of IκBα

In the present study, we performed immunoblotting analysis to investigate the mechanism of reducing TBHP-induced NF-κB activation in CSB treatment. We observed that exposure to TBHP increased the phosphorylation of IKK*α/β* as well as degraded I*κ*B*α* which ultimately help to translocate NF-*κ*B p65 in the nucleus. In addition, we also observed that TBHP decreased the expression of NF-*κ*B in the cytosol and time-dependently decreased the expression of I*κ*B*α* (beginning at 30 min) (Figures 6C–E). Incubation of the hepatocytes with CSB either prior to or simultaneous with the TBHP, however, could prevent the TBHP-induced nuclear translocation of NF-*κ*B p65 and phosphorylated IKK*α/β* as well as degradation of I*κ*B*α*.

Effect of CSB against TBHP-induced cell death pathway

To understand the nature of cell death, next we focused on the DNA fragmentation analysis. In Figure 7, it has been observed that TBHP exposure elevated the DNA fragmentation and caused DNA laddering which indicates the majority of the cell death via the apoptotic pathway. CSB treatment, however, could prevent the TBHP-induced DNA fragmentation, suggesting that CSB might prevent the TBHP-induced apoptotic cell death. In addition to DNA fragmentation analysis, a double labelling technique has been utilized using Annexin V/PI to distinguish between apoptotic and necrotic cells. In this process, fluorescence generated by Annexin binding to externalized phosphatidylserine of apoptotic cells indicates the apoptotic cell death. However, PI binding reflects the necrotic cell death as well. Annexin V/PI binding flow cytometric data (Figure 8) revealed that, in comparison with control untreated hepatocytes, TBHP increased the number of Annexin V staining hepatocytes but very little PI binding, indicating the majority of cells death via the apoptotic pathway which corroborates with the DNA fragmentation data. Treatment with CSB shows a smaller number of apoptotic cells, indicating that CSB treatment protected the TBHP-induced apoptotic cell death.

Effect on the Bcl-2 family of proteins and mitochondria dependent cell death pathway

Bcl-2 family proteins are upstream regulators of mitochondrial membrane potential. Figure 9A represents the expressions of Bcl-2 family of proteins. From immunoblotting studies, it has been observed that TBHP up-regulated pro-apoptotic (Bad) and down-regulated anti-apoptotic (Bcl-2) members of Bcl-2 family proteins and that could be prevented by the CSB treatment.

Oxidative stress-induced apoptotic cell death is directly related to mitochondrial dysfunction. Disruption of mitochondrial membrane potential, release of cytochrome C and activation of caspase 3 are the novel biomarkers of oxidative stress-induced cell death via a mitochondria-dependent pathway. Immunoblot analyses (Figure 9) showed that TBHP intoxication reduced the mitochondrial membrane potential (Figure 9B), elevated the concentration of cytosolic cytochrome C (Figure 9C) and up-regulated the cleaved caspase 3 (Figure 9D), indicating the involvement of the mitochondria-dependent signalling cascades in

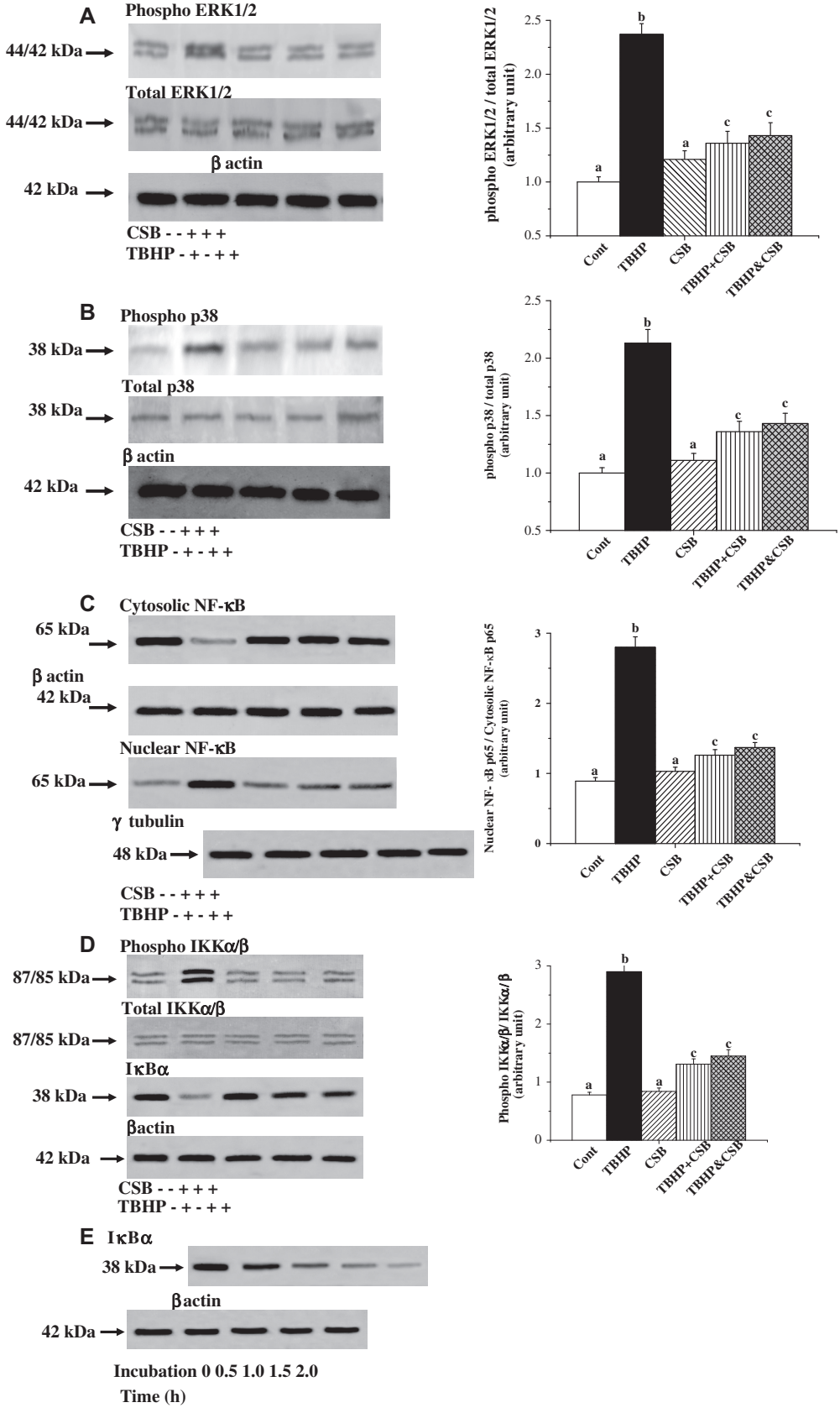

Figure 6. Western blot analysis of MAPKs and NF-κB. p38 (A); ERK1/2 (B); Cytosolic and Nuclear NF-κB (C); Phospho and total IKKα/β, IκBα (D); Time-dependent effect of IκBα (E), in the normal and experimental hepatocyte. The relative intensities of bands were determined using NIH-image software. Cont: normal hepatocytes, CSB: hepatocytes treated with CSB, TBHP: TBHP-exposed hepatocytes, CSB + TBHP: hepatocytes treated with CSB prior to TBHP addition and CSB&TBHP: hepatocytes exposed to CSB and TBHP simultaneously. Data are mean ± SD, for six sets per group and were analysed by one-way ANOVA, with Student-Newman-Keuls post-hoc tests. Differences were attributed at $p < 0.05$ and homogeneous sub-groups share common superscripted letters.

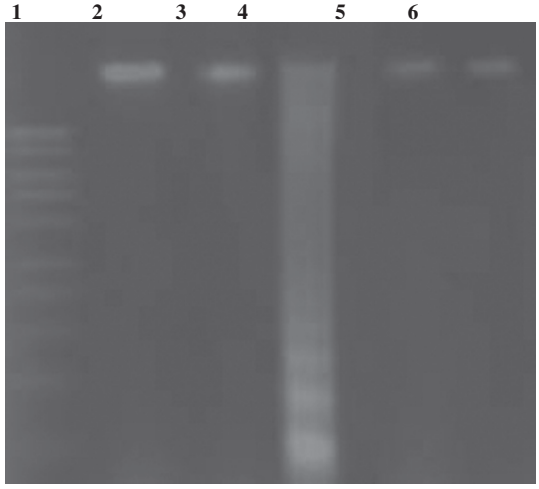

Figure 7. DNA fragmentation on agarose/ethydium bromide gel. DNA isolated from experimental hepatocytes was loaded onto 1% (w/v) agarose gels. Lane 1: Marker (1 kb DNA ladder); Lane 2: DNA isolated from normal hepatocytes; Lane 3: DNA isolated from CSB treated hepatocytes; Lane 4: DNA isolated from TBHP exposed hepatocytes; Lane 5: DNA isolated from hepatocytes treated with CSB prior to TBHP addition and Lane 6: DNA isolated from hepatocytes exposed to CSB and TBHP simultaneously.

this pathophysiology. Treatment with CSB either prior to or simultaneous with the toxin exposure prevented the TBHP-induced mitochondria-dependent cell death pathway.

Discussion

During the last few decades, interest in redox signalling studies has been significantly increased because of the involvement of reactive oxygen species (ROS) in cell growth, differentiation and death. ROS are usually known for their deleterious effects on macromolecules. Nucleic acids, proteins and membrane phospholipids are damaged by these active species [35]. Fortunately, cells are enriched with antioxidants, which can react with ROS and neutralize them before they inflict damage on vital components. Glutathione, ascorbic acid, α-tocopherol, thioredoxin and a number of antioxidant enzymes (like superoxide dismutase, glutathione peroxidase catalase, etc.) are the endogenous agents which can detoxify ROS [36]. However, when the endogenous antioxidant mechanisms are overwhelmed by ROS, oxidative stress occurs and ultimately leads to necrotic or apoptotic cell death [37]. To avoid this unwanted pathophysiology, supplementation of antioxidants from outside is, therefore, necessary.

Antioxidant as well as anti-inflamatory properties of various types of CSB have already been reported in the literature. However, little is known about the beneficial role of CSB in the organ pathophysiology. The present study was, therefore, designed to investigate the mode of action of a coumarin-derived anti-

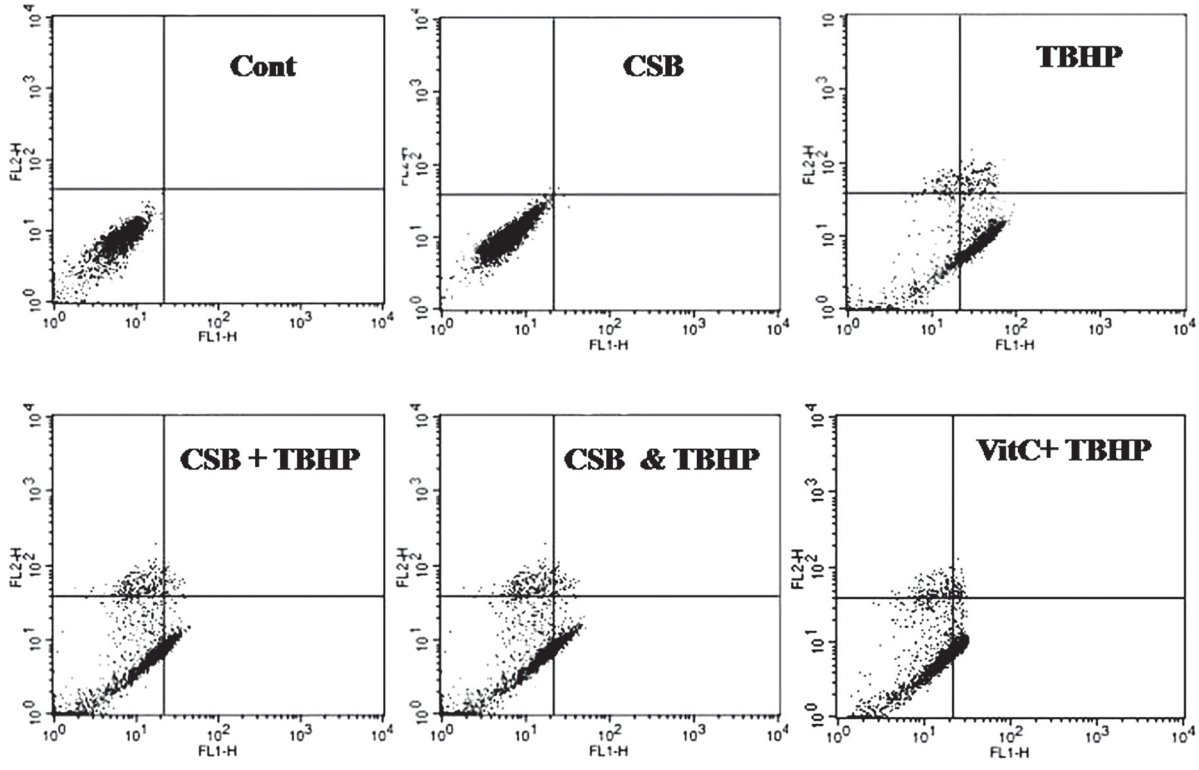

Figure 8. Effect of CSB and TBHP on percentage distribution of apoptotic and necrotic cells. Cell distribution analysed using Annexin V binding and PI uptake. The FITC and PI fluorescence measured using flow cytometer with FL-1 and FL-2 filters, respectively. Results expressed as dot plot representing as one of the six independent experiments. Cont: normal hepatocytes, CSB: hepatocytes treated with CSB, TBHP: TBHP-exposed hepatocytes, CSB + TBHP: hepatocytes treated with CSB prior to TBHP addition; CSB&TBHP: hepatocytes exposed to CSB and TBHP simultaneously and VitC + TBHP: hepatocytes treated with vitamin C prior to TBHP addition.

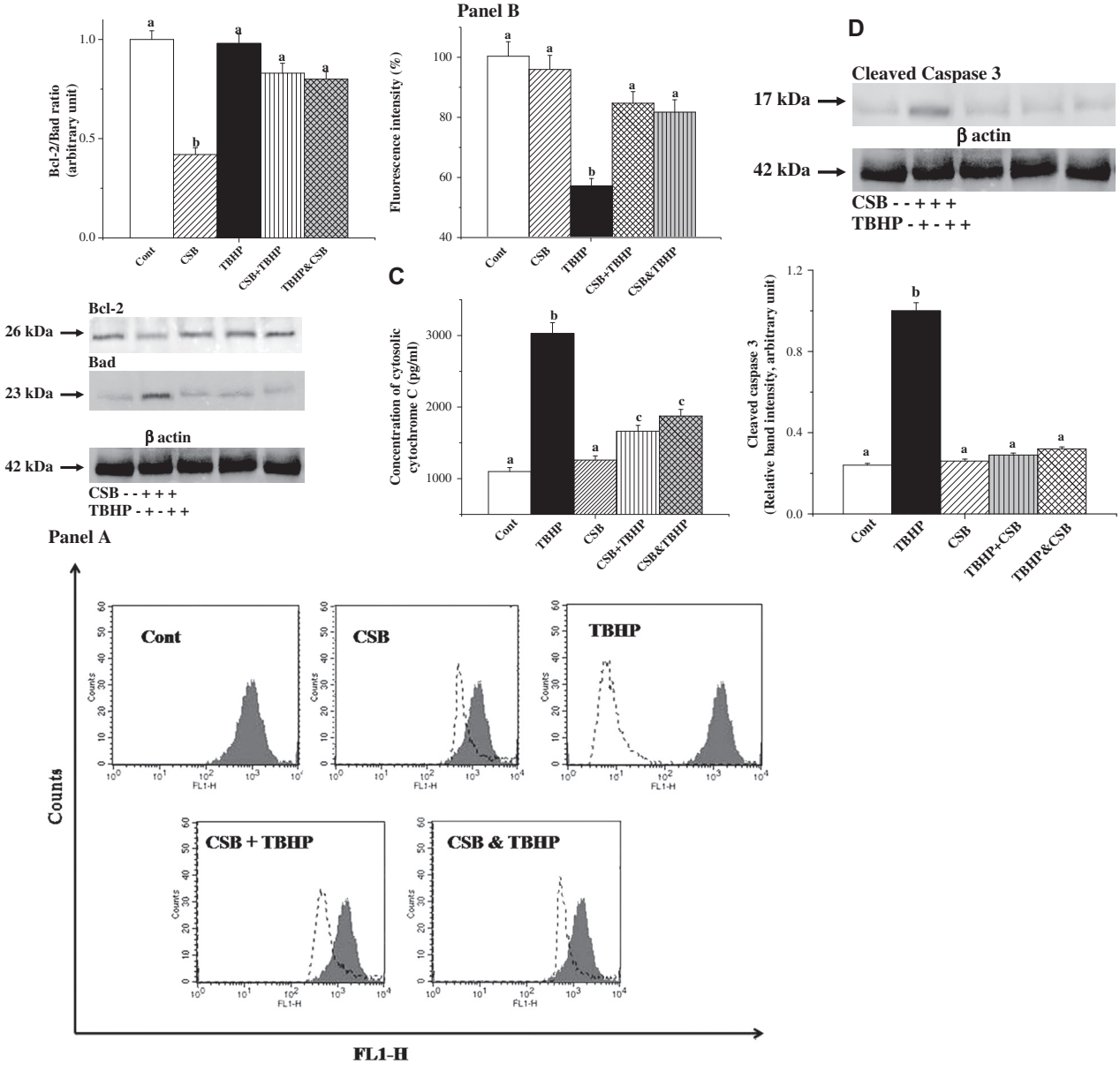

Figure 9. Western blot analysis of Bad and Bcl-2 (A); mitochondrial membrane potential (B); cytosolic cytochrome C (C) and the expression of cleaved caspase 3 (D) in the normal and experimental hepatocytes. The relative intensities of bands were determined using NIH-image software. Cont: normal hepatocytes, CSB: hepatocytes treated with CSB, TBHP: TBHP-exposed hepatocytes, CSB + TBHP: hepatocytes treated with CSB prior to TBHP addition and CSB&TBHP: hepatocytes exposed to CSB and TBHP simultaneously. Data are mean ± SD, for six sets per group and were analysed by one-way ANOVA, with Student-Newman-Keuls post-hoc tests. Differences were attributed at $p < 0.05$ and homogeneous sub-groups share common superscripted letters.

oxidant molecule (CSB) against TBHP-induced cell death and to identify the signalling molecules involved in this process.

The free radical scavenging property of a molecule helps it to prevent a system against oxidative insult. Thus, before going into the cellular system we first investigated the radical scavenging activity of CSB in the cell free system and found that CSB can effectively scavenge the free radicals like DPPH, super oxide, hydroxide, etc.

Cell viability is directly associated with the membrane integrity as well as the structure of the cell membrane. In the present study cellular damage was detected by measuring the percentage of cell viability as well as the activities of the membrane leakage enzymes, namely ALT and LDH. It has been observed that TBHP exposure reduced the percentage of cell viability and increased the activities of membrane leakage enzymes, ALT and LDH. TBHP-induced increased production of intracellular ROS was detected by the DCF formation. TBHP exposure increased the intracellular DCF production. Incubation of the hepatocytes with CSB both prior to and in combination with TBHP prevented the intracellular ROS production as well as loss in cell viability and kept the activities of ALT and LDH almost close to that of normal.

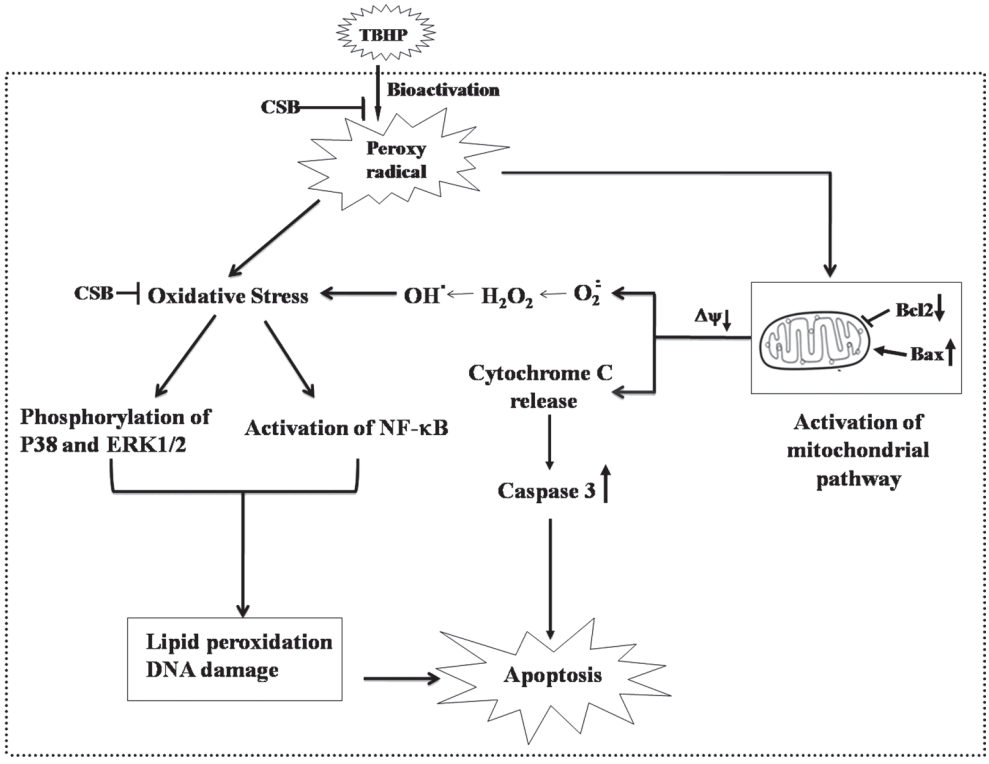

Figure 10. Schematic diagram of the protective role of CSB against TBHP-induced oxidative stress-induced signalling cascades.

Antioxidant enzymes are considered to be the first line of cellular defence which prevents the cellular ingredients from oxidative damage. Among the antioxidant enzymes, SOD and CAT are the most important enzymes against the toxic effects of oxygen metabolism. SOD quenches O_2^- into the corresponding H_2O_2 and H_2O [38]. CAT accelerates the dismutation reaction of H_2O_2 followed by the formation of H_2O and O_2 [39]. GR and GPx also maintain the intracellular redox status [40]. Thus, to eliminate free radicals, these cellular antioxidant enzymes play an important role. Under normal physiological conditions, equilibrium exists between these enzymes. However, this equilibrium is lost when the rate of production of intracellular ROS overwhelms the rate of elimination and consequently established the oxidative insult. In the present study, TBHP exposure caused reduction in the activities of antioxidant enzymes in the experimental hepatocytes compared to normal and that alteration could be prevented by CSB treatment.

The glutathione-based antioxidant system plays a second line of cellular defense against ROS and other oxidant species [41]. The levels of GSH, GSSG and total thiols are additional indicators of oxidative injury. During the metabolic action of GSH, its sulphydryl group becomes oxidized, resulting with the formation of corresponding disulphide compound, GSSG (oxidized form). Thus, depletion of GSH content is associated with an increase in GSSG concentration, resulting with the depletion in GSH/GSSG ratio. In the present study following TBHP intoxication, cellular glutathione redox status was greatly impaired, as indicated by a significant decrease in the levels of GSH along with the increased level of its metabolite GSSG. Per oxidative damage of the membrane polyunsaturated fatty acids plays an important role in the generation of cellular damage in TBHP-toxicity. It has been observed that TBHP intoxication induced a marked increased in the MDA (a stable metabolite of the free radical-mediated lipid peroxidation cascade) as well as protein carbonyl level. Results of our study suggest that either pre- or simultaneous incubation of CSB decreased the level of TBHP-induced enhanced GSSG, normalized the GSH/GSSG ratio and also reduced the lipid peroxidation as well as protein carbonylation.

Oxidative stress induces the transcription of a variety of genes involved in the detoxification of ROS or in the repair of ROS-induced damage. Increased production of ROS activates the redox sensitive transcription factors (TFs) induced signal transduction pathways which in turn leads to transcription of genes involved in the cell growth regulatory pathways. Among many transcription factors, NF-κB (nuclear factor κB) is known to be a rapidly induced stress-responsive one. NF-κB has been implicated in the gene regulation, related to cell proliferation, apoptosis, adhesion, immune and inflammatory responses [42]. Phosphorylation at the multiple serine sites of p65 sub-unit increases the transcriptional activity of NF-κB in the nucleus where it binds to the DNA and induces gene expression [43].

Normally NF-κB resides in the cytoplasm and is inhibited to translocate into the nucleus due to complex formation with its inhibitory sub-unit IkBα. Activation of NF-κB is mediated via degradation of IkBα which occurred primarily via the activation of IKK (phosphorilation of IKKα/β). In the present study, we observed that TBHP exposure caused activation of NF-κB (p65 sub-unit), phosphorylation of IKKα/β and degradation of IκBα and that could be inhibited by the CSB treatment. Besides, NF-κB can serve as a target of MAP kinases (p38, ERK1/2 and JNK) [44,45] belonging to a class of redox-signalling molecules sharing a common Thr–X–Tyr site in the activation loop and Thr–Tyr phosphorylation for the initiation of kinase activity. The three MAPKs transduce intra- and extra-cellular stimuli, which lead to diverse cellular responses. The ERK1/2 pathway typically responds to the growth factor signals, which leads to cell differentiation or proliferation. In contrast, the JNK and p38 pathways respond to cytokines and cellular stress; resulting in the transcriptional activation of genes involved in stress responses, growth arrest or apoptosis.

ERKs, JNKs and p38 kinases have been shown to be activated in response to oxidant injury in various cell types including hepatocytes [46]. A number of investigators have also shown that p38 and ERK1/2 MAPKs play a role in inducing cellular toxicity in oxidative stress responsive hepatocytes [47,48]. Therefore, in the present study we have investigated the role of p38, JNK and ERK1/2 MAPKs and observed that TBHP exposure caused activation of phosphorylated ERK1/2 as well as phosphorylated p38, leaving the activation of phosphorylated JNK unchanged. These observations help us to conclude that p38 and ERK1/2 MAPKs play a pro-apoptotic role in this pathophysiology. Results clearly showed that incubation with CSB either prior to or in combination with TBHP prevented the activation of phosphorylated ERK1/2 as well as phosphorylated p38.

DNA gel electrophoresis revealed that exposure to TBHP elevated the chromatin condensation as well as DNA fragmentation, which appeared as DNA laddering in the agarose-ethydium bromide gel electrophoresis. The result of this study clearly indicates TBHP-induced cell death via apoptotic pathway. FACS analysis with Annexin V/PI double staining also showed increased population of apoptotic cell death in TBHP exposed cells. Being an antioxidant, CSB prevented the TBHP-induced DNA fragmentation and apoptotic cell death.

Apoptosis is known to be a delicately controlled programmed cell death pathway. Cumulative evidences suggest that the alteration in mitochondrial membrane potential is able to switch the committed cells to apoptotic death via oxidative stress responsive signalling cascades [49,50], reporting the influence of Bcl-2 family proteins on the mitochondria to regulate the mitochondria-dependent cell death. There are two classes of reciprocal regulatory proteins in the Bcl-2 family: the anti-apoptotic members (e.g. Bcl-2, Bcl-xL) protect the cells from apoptosis, whereas the pro-apoptotic members (e.g. Bax, Bad) promote the programmed cell death. Action of Bcl-2 family proteins on mitochondria causes the release of cytochrome C from mitochondria to the cytosol. In the cytosol, cytochrome C interacts with Apaf1 and procaspase-9 to form the apoptosome that triggers the activation of caspase-3. In our study we observed that, in agreement with the DNA fragmentation and FACS analysis, TBHP exposure up-regulated the pro-apoptotic (Bad) and down-regulated anti-apoptotic (Bcl-2) members of Bcl-2 proteins. Alteration in the Bcl-2/Bad ratio caused reduction in mitochondrial membrane potential, release of cytochrome C and subsequently activated the cell death executor caspases (e.g. cleaved caspase 3). CSB treatment, however, prevented TBHP-induced alteration in the Bcl-2/Bad ratio and mitochondria-dependent cell death.

In conclusion we would like to state that incubation of hepatocytes with TBHP caused an alteration in the cellular antioxidant status and induced apoptic cell death via mitochondrial dependent as well as independent pathways. Treatment with CSB both prior to or in combination with the TBHP kept that antioxidant status quite similar to that of normal and prevented the apoptotic signalling pathways. The radical scavenging activity of CSB mainly helps the molecule to prevent the TBHP-induced oxidative insult and cell death (Figure 10). However, further studies are necessary to investigate the prophylactic role of CSB in oxidative stress-induced organ pathophysiology.

Acknowledgement

The authors are grateful to Mr Prasanta Pal for his excellent technical assistance for the study.

Declaration of interest

The authors report no conflicts of interest. The authors alone are responsible for the content and writing of the paper.

References

[1] Bruneton J. Pharmacognosy, medicinal plants. 2nd ed. Paris: Lavoisier Publishing; 1999. p. 225–459.
[2] Murray RDH. Coumarins. Nat Prod Rep 1989;8:591–624.
[3] Farombi EO, Nwaokeafor IA. Anti-oxidant mechanisms of kolaviron: studies on serum lipoprotein oxidation, metal chelation and oxidative membrane damage in rats. Clin Exp Pharmacol Physiol 2005;32:667.
[4] Laurin P, Ferroud D, Klich M, Dupis-Hamlin C, Mauvais P, Lassaigne P, Bonnefoy A, Musicki B. Synthesis and *in vitro*

evaluation of novel highly potent coumarin inhibitors of gyrase. Bioorg Med Chem Lett 1999;9:2079–2084.
[5] Emmanuel-Giota AA, Fylaktakidou KC, Hadjipavlou-Litina DJ, Litinas KE, Nicolaides DN. Synthesis and biological evaluation of several 3-(coumarin-4-yl)tetrahydroisoxazole and 3-(coumarin-4-yl)dihydropyrazole derivatives. J Heterocyclic Chem 2001;38:717–722.
[6] Azza AA, Abu-Hussen. Synthesis and spectroscopic studies on ternary bis-Schiff-base complexes having oxygen and/or nitrogen donors. J Coord Chem 2006;59:157–176.
[7] Singh K, Barwa MS, Tyagi P. Synthesis, characterization and biological studies of Co(II), Ni(II), Cu(II) and Zn(II) complexes with bidentate Schiff bases derived by heterocyclic ketone. Eur J Med Chem 2006;41:147–153.
[8] Mladenova R, Ignatova M, Manolova N, Petrova T, Rashkov I. Preparation, characterization and biological activity of Schiff base compounds derived from 8-hydroxyquinoline-2-carboxaldehyde and Jeffamines ED. Eur Polym J 2002;38:989–999.
[9] Melagraki G, Afantitis A, Igglessi-Markopoulou O, Detsi A, Koufaki M, Kontogiorgis C, Hadjipavlou-Litina DJ. Synthesis and evaluation of the antioxidant and anti-inflammatory activity of novel coumarin-3-aminoamides and their alpha-lipoic acid adducts. Eur J Med Chem 2009;44:3020–3026.
[10] Kontogiorgis CA, Hadjipavlou-Litina DJ. Synthesis and biological evaluation of novel coumarin derivatives with a 7-azomethine linkage. Bioorg Med Chem Lett 2004;14:611–614.
[11] Kontogiorgis CA, Hadjipavlou-Litina DJ. Synthesis and anti-inflammatory activity of coumarin derivatives. J Med Chem 2005;48:6400–6408.
[12] Cawthon D, McNew R, Beers KW, Bottje WG. Evidence of mitochondrial dysfunction in broilers with pulmonary hypertension syndrome (Ascites): effect of t-butyl hydroperoxide on hepatic mitochondrial function, glutathione, and related thiols. Poult Sci 1999;78:114–124.
[13] Kaur P, Kaur G, Bansal MP. Upregulation of AP1 by tertiary butylhydroperoxide induced oxidative stress and subsequent effect on spermatogenesis in mice testis. Mol Cell Biochem 2008;308:177–181.
[14] Tarín JJ, Pérez-Albalá S, García-Pérez MA, Cano A. Effect of dietary supplementation with a mixture of Vitamins C and E on fertilization of tertiary butyl hydroperoxide-treated oocytes and parthenogenetic activation in the mouse. Theriogenology 2002;57:869–881.
[15] Spector A, Ma W, Sun F, Li D, Kleiman NJ. The effect of H_2O_2 and tertiary butyl hydroperoxide upon a murine immortal lens epithelial cell line, alpha TN4-1. Exp Eye Res 2002;75:573–582.
[16] Kennedy CH, Church DF, Winston GW, Pryor WA. Tert-Butylhydroperoxide induced radical production in rat liver mitochondria. Free Radic Biol Med 1992;12:381–387.
[17] Guidarelli A, Clementi E, Sciorati C, Cattabeni F, Cantoni O. Calcium-dependent mitochondrial formation of a species mediating DNA single strand breakage in U937 cells exposed to sub-lethal concentrations of tert-butyl-hydroperoxide. J Pharmacol Exp Ther 1997;283:66–74.
[18] Sarkar MK, Sil PC. Prevention of tertiary butyl hydroperoxide induced oxidative impairment and cell death by a novel antioxidant protein molecule isolated from the herb, Phyllanthus niruri. Toxicol In Vitro 2010;24:1711–1719.
[19] Sarkar MK, Kinter M, Mazumder B, Sil PC. Purification and characterisation of a novel antioxidant protein molecule from Phyllanthus niruri. Food Chem 2009;114:1405–1412.
[20] Gacche RN, Gond DS, Dhole NA, Dawane BS. Coumarin Schiff-bases: as antioxidant and possibly anti-inflammatory agents. J Enz Inhib Med Chem 2006;21:157–161.
[21] Blois MS. Antioxidant determination by use of a stable free radical. Nature 1958;29:1199–1200.
[22] Nash T. The colorimetric estimation of formaldehyde by means of the Hantzsch reaction. J Biochem 1953;55:416–421.
[23] Siddhuraju P, Becker K. Antioxidant properties of various solvent extracts of total phenolic constituents from three different agroclimatic origins of drumstick tree (Moringa oleifera Lam.) leaves. J Agric Food Chem 2003;51:2144–2155.
[24] Sarkar K, Sil PC. A 43kDa protein from the herb Cajanus indicus L. Protects thioacetamide induced cytotoxicity in hepatocytes. Toxicol In Vitro 2006;20:634–640.
[25] Hansen MB, Nielsen SE, Berg K. Re-examination and further development of a precise and rapid dye method for measuring cell growth/cell kill. J Immunol Methods 1989;119:203–210.
[26] Bradford MM. A rapid and sensitive method for the quantitation of microgram quantities of protein utilizing the principle of protein-dye binding. Anal Biochem 1976;72:248–254.
[27] LeBel CP, Bondy SC. Sensitive and rapid quantitation of oxygen reactive species formation in rat synaptosomes. Neurochem Int 1990;17:435–440.
[28] Kim JD, McCarter RJM, Yu BP. Influence of age, exercise and dietary restriction on oxidative stress in rats. Aging Clin Exp Res 1996;8:123–129.
[29] Esterbauer H, Cheeseman KH. Determination of aldehydic lipid peroxidation products: malonaldehyde and 4-hydroxynonenal. Methods Enzymol 1990;186:407–421.
[30] Uchida K, Stadtman ER. Covalent attachment of 4-hydroxynonenal to glyceraldehydes-3-phosphate dehydrogenase. J Biol Chem 1993;268:6388–6393.
[31] Sinha M, Manna P, Sil PC. Taurine, a conditionally essential amino acid, ameliorates arsenic-induced cytotoxicity in murine hepatocytes. Toxicol In Vitro 2007;21:1419–1428.
[32] Ji L, Liu T, Chen Y, Wang Z. Protective mechanisms of N-acetyl-cysteine against pyrrolizidine alkaloid clivorine-induced hepatotoxicity. J Cell Biochem 2009;108:424–432.
[33] Tapalaga D, Tiegs G, Angermüller S. NFkB and caspase-3 activity in apoptotic hepatocytes of galactosamine-sensitized mice treated with TNFα . J Histochem Cytochem 2002;50:1599–1609.
[34] Mingatto FE, Rodrigues T, Pigoso AA, Uyemura SA, Curti C, Santos AC. The critical role of mitochondrial energetic impairment in the toxicity of nimesulide to hepatocytes. J Pharm Exp Therap 2003;303:601–607.
[35] McCord JM. The evolution of free radicals and oxidative stress. Am J Med 2000;108:652–659.
[36] Halliwell B. Antioxidants in human health and disease. Annu Rev Nutr 1996;16:33–50.
[37] Chandra J, Samamli A, Orrenius S. Triggering and modulation of apoptosis by oxidative stress. Free Radic Biol Med 2000;29:323–333.
[38] Fridovich I. Superoxide radical and superoxide dismutase. Acc Chem Res 1972;5:321–323.
[39] Jones P, Suggett A. The catalase–hydrogen peroxide system. A theoretical appraisal of the mechanism of catalase action. Biochem J 1968;110:621–629.
[40] Ketterer B. Detoxification reactions of glutathione and glutathione reductase. Xenobiotca 1986;16:957–975.
[41] Rosenblat M, Aviram M. Macrophase glutathione content and glutathione peroxidase activity are inversely related to cell-mediated oxidation of LDL: *in vitro* and *in vivo* studies. Free Radic Biol Med 1998;24:305–317.
[42] Baldwin AS. The NF-kappa B and I kappa B proteins: new discoveries and insights. Annu Rev Immunol 1996;14:649–683.
[43] Akira S, Kishimoto T. NF-IL6 and NF-kB in cytokine gene regulation. Adv Immunol 1997;65:1–46.

[44] Cowan KJ, Storey KB. Mitogen-activated protein kinases: new signalling pathways functioning in cellular responses to environmental stress. J Exp Biol 2003;206:1107–1115.
[45] Yang SH, Sharrocks AD, Whitmarsh AJ. Transcriptional regulation by the MAP kinase signaling cascades. Gene 2003;320: 3–21.
[46] Song MO, Freedman JH. Activation of mitogen activated protein kinases by PCB126 (3,3', 4,4', 5-Pentachlorobiphenyl) in HepG2 Cells. Toxicol Sci 2005;84:308–318.
[47] Wu D, Cederbaum AI. Role of p38 MAPK in CYP2E1-dependent Arachidonic acid toxicity. J Biol Chem 2003;278: 1115–1124.

This paper was first published online on Early Online on 18 March 2011.

[48] Mohamed A, Abdelmegeed MA, Kim SK, Woodcroft KJ, Novak RF. Acetoacetate activation of extracellular signal-regulated kinase 1/2 and p38 mitogen-activated protein kinase in primary cultured rat hepatocytes: role of oxidative stress. JPET 2004;310:728–736.
[49] Keeble JA, Gilmore AP. Apoptosis commitment–translating survival signals into decisions on mitochondria. Cell Res 2007;17:976–984.
[50] Verzola D, Bertolotto MB, Villaggio B, Ottonello L, Dallegri F, Frumento G, Berruti V, Gandolfo MT, Garibotto G, Deferran G. Taurine prevents apoptosis induced by high glucose in human tuble renal cells. J Investig Med 2002;50:443–451.